Neuro-Oncology

Neuro-Oncology 16(8), 1057–1066, 2014
doi:10.1093/neuonc/not317
Advance Access date 26 January 2014

Treatment of orthotopic malignant peripheral nerve sheath tumors with oncolytic herpes simplex virus

Slawomir Antoszczyk, Melanie Spyra, Victor Felix Mautner, Andreas Kurtz, Anat O. Stemmer-Rachamimov, Robert L. Martuza, and Samuel D. Rabkin

Department of Neurosurgery, Massachusetts General Hospital and Harvard Medical School, Boston, Massachusetts (S.A., R.L.M., S.D.R.); Department of Pathology, Massachusetts General Hospital and Harvard Medical School, Boston, Massachusetts (A.O.S.R.); Department of Neurology, University Medical Center Hamburg-Eppendorf, Hamburg, Germany (M.S., V.F.M.); Berlin-Brandenburg Center for Regenerative Therapies, Charité Medical University, Berlin, Germany (A.K.); College of Veterinary Medicine, Seoul National University, Seoul, Korea (A.K.)

Corresponding Author: Samuel D. Rabkin, PhD, Molecular Neurosurgery Laboratory, Department of Neurosurgery, MGH-Simches, 185 Cambridge St., CPZN-3800, Boston, MA 02114 (rabkin@helix.mgh.harvard.edu).

Backgrounds. Malignant peripheral nerve sheath tumors (MPNSTs) are an aggressive and often lethal sarcoma that frequently develops in patients with neurofibromatosis type 1 (NF1). We developed new preclinical MPNST models and tested the efficacy of oncolytic herpes simplex viruses (oHSVs), a promising cancer therapeutic that selectively replicates in and kills cancer cells.

Methods. Mouse NF1$^-$ MPNST cell lines and human NF1$^-$ MPNST stemlike cells (MSLCs) were implanted into the sciatic nerves of immunocompetent and athymic mice, respectively. Tumor growth was followed by external measurement and sciatic nerve deficit using a hind-limb scoring system. Oncolytic HSV G47Δ as well as "armed" G47Δ expressing platelet factor 4 (PF4) or interleukin (IL)-12 were injected intratumorally into established sciatic nerve tumors.

Results. Mouse MPNST cell lines formed tumors with varying growth kinetics. A single intratumoral injection of G47Δ in sciatic nerve tumors derived from human S462 MSLCs in athymic mice or mouse M2 (37-3-18-4) cells in immunocompetent mice significantly inhibited tumor growth and prolonged survival. Local IL-12 expression significantly improved the efficacy of G47Δ in syngeneic mice, while PF4 expression prolonged survival. Injection of G47Δ directly into the sciatic nerve of athymic mice resulted in only mild symptoms that did not differ from phosphate buffered saline control.

Conclusions. Two new orthotopic MPNST models are described, including in syngeneic mice, expanding the options for preclinical testing. Oncolytic HSV G47Δ exhibited robust efficacy in both immunodeficient and immunocompetent MPNST models while maintaining safety. Interleukin-12 expression improved efficacy. These studies support the clinical translation of G47Δ for patients with MPNST.

Keywords: cancer stem cells, HSV, IL-12, MPNST, neurofibromatosis, sciatic nerve, virotherapy.

Malignant peripheral nerve sheath tumors (MPNSTs) are rare, highly aggressive soft-tissue sarcomas arising in peripheral nerves, with very poor prognosis and resistance to traditional chemotherapy or radiation.[1,2] The current standard of care is surgical resection, which is often incomplete or accompanied by significant loss of function, in conjunction with radiotherapy and/or chemotherapy, for which the benefits are inconclusive.[1,3] About 50% of MPNSTs develop in patients with neurofibromatosis type 1 (NF1), a frequently occurring autosomal dominant genetic disease, which affects about 1:4000 births.[2,4–6] The NF1 gene product, neurofibromin, contains a Ras-GTPase activating protein domain that negatively regulates Ras activity.[7] In MPNST, loss of heterozygosity of NF1 occurs, with tumors that have constitutively activated Ras.[8]

Because of the relative rarity of MPNST and the limited patient population compared with other cancers, it is difficult to conduct randomized controlled clinical trials or to evaluate the increasing number of potential therapeutic agents in patients. Therefore, preclinical models are very important in identifying and prioritizing agents for clinical translation. A number of genetically engineered mouse models have been developed in which high-grade peripheral nerve sheath tumors arise that are histologically similar to human MPNSTs.[9] This includes the initial cis-linked Nf1$^{+/-}$/Trp53$^{+/-}$ model.[10,11] MPNST cells isolated from tumors arising in

Received 22 August 2013; accepted 18 December 2013

these mice have been used as models in immunodeficient mice, but not in immunocompetent mice until now.[12,13]

An additional avenue for preclinical modeling takes advantage of cancer stem cells that have been isolated from a number of solid tumors, often by sphere formation in serum-free media with growth factors,[14] including from a variety of sarcomas.[15–19] We recently established MPNST stemlike cells (MSLCs) from a human MPNST cell line.[20] These MSLCs form spheres in media with epidermal growth factor (EGF) and basic fibroblast growth factor (FGF) that can self-renew, form secondary spheres from single cells, express stem cell markers, and differentiate into multiple lineages in serum or lineage-specific growth factors.[20] Here we describe a new orthotopic tumor model generated from sciatic nerve implantation of these human MSLCs.

Oncolytic herpes simplex viruses (oHSVs) are genetically engineered to replicate selectively in cancer cells—killing them, generating more virus, and spreading within the tumor.[21] In addition to direct cell killing, oHSV also induces a robust antitumor immune response.[22] Oncolytic HSVs, containing a variety of mutations, have proven very effective in treating tumors in mouse models.[21,23] This has led to a number of clinical trials, including a phase III trial for melanoma.[24] Because of their size, oHSV can be "armed" with therapeutic transgenes—including immunomodulatory, anti-angiogenic, and cytotoxic genes—that are expressed in the tumor after infection.[25,26] In these studies we use G47Δ, a third-generation oHSV[27] that is efficacious in treating nervous system tumors and cancer stem cells.[28–30] To enhance activity, G47Δ has been "armed" with interleukin (IL)-12 or platelet factor 4 (PF4).[13,31] Interleukin-12 is a heterodimeric proinflammatory cytokine that promotes type 1 T helper cell immune responses, interferon (IFN)-γ production, and anti-angiogenesis.[32] PF4 (CXCL4), a heparin-binding tetramer, inhibits angiogenesis and the binding of growth factors (FGF and vascular endothelial growth factor) to their receptors and activates natural killer cells and nonspecific antitumor immune responses.[33,34] We previously reported that G47Δ-PF4 inhibited the growth of subcutaneous M2 MPNSTs in immunodeficient mice.[13]

In this study, we describe 2 new orthotopic sciatic nerve MPNST models: (i) mouse MPNST cell lines derived from spontaneously arising tumors in transgenic mice implanted into immunocompetent mice and (ii) human MSLCs implanted into immunodeficient mice. This is the first report of an MSLC tumor model and an immunocompetent MPNST implant model. G47Δ was very effective at treating both tumor models, and arming oHSV with IL-12 or PF4 improved activity in immunocompetent mice.

Materials and Methods

Cells and Viruses

Mouse MPNST cells derived from spontaneously arising tumors in Nf1/Trp53 heterozygous mice were obtained from the Luis Parada Lab (University of Texas Southwestern Medical School)[10] and cultured in Dulbecco's modified Eagle's medium (DMEM; Cellgro), 10% fetal calf serum (HyClone), streptomycin (100 μg/mL), and penicillin (100 U/mL; Cellgro) as monolayers at 37°C in an atmosphere of 5% CO_2. We have renamed the cells for ease of identification: M1 = 61E4, M2 = 37-3-18-4, M3 = 35-1-2, M4 = 38-2-18, M5 = 39-2-11, and M6 = 32-5-24-12. Some of these have been previously described.[35,36] Human S462 MSLCs[20] were cultured in Neurobasal media supplemented with 3 mM L-Glutamine (Mediatech), B27 supplement (Invitrogen), N2 supplement (Invitrogen), 2 μg/mL heparin (Sigma), 20 ng/mL recombinant human EGF (R & D systems), 20 ng/mL recombinant human FGF2 (Peprotech), and 0.5× penicillin G/streptomycin sulfate/amphotericin B complex (Mediatech), in ultra-low attachment flasks (Corning) at 37°C in an atmosphere of 5% CO_2. All cells were used at low passage number and confirmed to be mycoplasma free (LookOut Mycoplasma kit, Sigma). Grown, purified, and titered on Vero cells (obtained from American Type Culture Collection) were oHSVs G47Δ (γ34.5Δ, ICP6$^-$, ICP47Δ, LacZ$^+$), G47Δ-empty (no transgene), armed G47Δ-mCherry (expressing mCherry), G47Δ-PF4 (expressing PF4), and G47Δ–IL12 (expressing IL-12) as previously described.[37] Armed oHSVs (Supplementary Fig. S1) were constructed using the Flip-Flop HSV bacterial artificial chromosome system[38] as previously described.[13,31]

Animal Models

All in vivo procedures were approved by the Subcommittee on Research Animal Care at Massachusetts General Hospital. For subcutaneous tumors, mouse MPNST cells were implanted into the flanks of female C57BL6/129SVSVImJ hybrid mice ∼8 weeks old (Jackson Laboratory); tumor sizes were measured and mice euthanized when tumor size exceeded 15 mm in diameter or tumors became ulcerated. For the orthotopic sciatic nerve models, mouse MPNST cells (5×10^4 in 2 μL) or human S462 MSLCs (1×10^5 in 2 μL) were implanted into the surgically exposed left sciatic nerve of female C57BL6/129SVSVImJ mice (as described) or female athymic mice ∼8 weeks old (NCI-Frederick), respectively, using a 30G needle and 10-μL Hamilton syringe. To evaluate tumor growth, left hind-limb function was evaluated twice a week using a neurologic scoring system we developed, measuring 5 parameters scored from 0 (abnormal) to 2 (normal) as illustrated in Supplementary Fig. S4. For the safety study, G47Δ or phosphate buffered saline (PBS) was injected directly into the sciatic nerve of non–tumor bearing athymic mice. Mice were weighed and their neurologic scores determined. At indicated days, mice were sacrificed and perfused with fixative (see Histology).

Treatment of Sciatic Nerve Tumors

At a time when tumors were established (typically when neurologic deficit was exhibited; as in Fig. 3A), mice were randomized into groups and virus treatment initiated (day 0). The tumor-bearing sciatic nerve was surgically exposed, and virus (dose indicated in legend) or PBS in 2 μL was injected using an intracranial catheter (Braintree Scientific) and syringe pump (80 μL/h). In some cases, tumors were treated with 2 injections. Tumor measurements were performed every 3–4 days with calipers; tumor volume (mm^3) = $\text{width}^2 \times \text{length}/2$. Mice were sacrificed when tumors reached 18 mm in maximal diameter or mice were unable to reach food or water.

Histology and X-Gal Staining

Tumors were removed after intracardiac perfusion (ice cold PBS, pH 7.3 [Cellgro]) followed by fixative (2% paraformaldehyde, 5 mM EDTA, 2 mM $MgCl_2$ in 0.1 M piperazine-N,N′-bis(2-ethanesulfonic acid), pH 7.3 [Calbiochem]), then were placed in fixative for an additional hour and submersed with cold PBS overnight. For X-Gal staining en bloc, tumors were incubated with X-Gal (Cellgro) 1 mg/mL, 5 mM potassium ferricyanide, 5 mM potassium ferrocyanide, 2 mM $MgCl_2$, 0.01% sodium deoxycholate (Sigma), and 0.02% NP-40 (nonyl phenoxypolyethoxylethanol; Sigma) in PBS, pH 7.3, for 3 h at 32°C. For sectioning, tumors were washed 30 s in H_2O at room temperature, 15 min in PBS at 32°C, 5 min in H_2O at 32°C, and 30 min in PBS at 4°C, submersed in 30% sucrose/2 mM $MgCl_2$ in PBS overnight at 4°C, and frozen in optimal cutting temperature compound (OCT; Sakura Finetek), and 20-μm sections were obtained with a Leica CM300 cryostat microtome. Sections were stained again with

X-Gal solution and counterstained with hematoxylin and eosin (Fisher Scientific). In some cases, tumors were removed and fixed in 4% paraformaldehyde (Electron Microscopy Sciences), then 30% sucrose in PBS overnight at 4°C, frozen in OCT, and prepared in 20-μm sections.

Electron Microscopy

Nerves, immediately after excision, were placed into electron microscopy fixative (2.5% glutaraldehyde, 2.0% paraformaldehyde, 0.025% calcium chloride in a 0.1 M sodium cacodylate buffer, pH 7.4) for 3 h at room temperature and then placed in cacodylate buffer. The nerves were postfixed with osmium tetroxide, en bloc stained with 2.0% uranyl acetate, dehydrated in a graded ethanol series, embedded in pure epoxy resin, and polymerized overnight at 60°C in a Leica Lynx automatic tissue processor. For light microscopy, 1-μm-thick sections were cut using glass knives and a Sorvall MT-1 (Dupont) ultramicrotome, floated on water droplets on glass slides, and dried in a humidity chamber on a warm hot plate. Toluidine blue stain (0.5% toluidine blue in aqueous 0.5% sodium borate) was pipetted over the sections and placed onto the hot plate until a slight gold rim could be seen around the stain droplet. The sections were rinsed in a stream of distilled water, dried, coverslipped, and examined. Representative nerves were chosen, the blocks trimmed, and thin sections, 0.25 μm, were cut using a diamond knife and an LKB 2088 ultramicrotome and placed on copper grids. Sections were stained with lead citrate and examined in a transmission electron microscope (FEI Morgagni). Images were captured with a 2K digital charge-coupled camera (Advanced Microscopy Techniques).

Statistical Analysis

We used Microsoft Excel and GraphPad Prism for statistic analysis. Tumor size and neurologic scores were compared using a 2-tailed Student's *t*-test (unpaired). Survival was analyzed using Kaplan–Meier curves compared by a log-rank (Mantel–Cox) test.

Results

Sciatic Nerve MPNST Model

We have established 2 nerve sheath tumor models: (i) mouse MPNST cell lines derived from spontaneously arising tumors in Nf1/Trp53 heterozygous transgenic mice implanted into immunocompetent C57BL6/129SVSVImJ hybrid mice and (ii) human MSLCs implanted into immunodeficient mice. We compared the growth of 6 mouse MPNST cell lines after subcutaneous and intrasciatic nerve implantation (Fig. 1). While fewer cells were implanted into the sciatic nerve, the rate of growth was similar to that seen after subcutaneous implantation, except that M5 was extremely slow and M3 was more rapid and comparable to M6 in the sciatic nerve (Fig. 1A and B). A representative M2 sciatic nerve tumor at day 23, along with the normal sciatic nerve in the right hind limb, is illustrated in Fig. 1D. Histological analysis of M2 and M3 tumors showed malignant poorly differentiated tumors composed of anaplastic cells with prominent nucleoli, often arranged in fascicles, with features of sarcoma (Supplementary Fig. S2). Previously we reported that M1 and M2, forming the most rapidly growing tumors, had high Ras activation, in contrast to M3–M5, with low Ras activation.[36] Human MSLCs also formed tumors after implantation into the sciatic nerve, but at a much slower rate than the mouse MPNST cells (Figs. 1E and 3B). Human MSLC tumors were poorly differentiated and highly mitotic and diffusely infiltrated along nerve axons (Supplementary Fig. S3). As would be expected, mice developed neurologic deficits as the tumors grew. To quantify this, we developed a neurologic scoring system of hind-limb function, which allowed us to follow the clinical consequences of tumor growth and treatment (Supplementary Fig. S4). The neurologic deficit typically arose before the tumor was detectable by external measurement (Figs. 3, 5, and 7) and therefore provided a useful measure of when tumors were established and when therapy could be initiated.

G47Δ Treatment of Human MSLC-derived Tumors

To examine G47Δ replication and spread in MSLCs, we infected S462 MSLC spheres with G47Δ-mCherry and followed virus spread in vitro by fluorescence microscopy. S462 spheres were permissive to oHSV infection, and virus efficiently spread throughout the spheres (Fig. 2A). To evaluate G47Δ efficacy in vivo, human

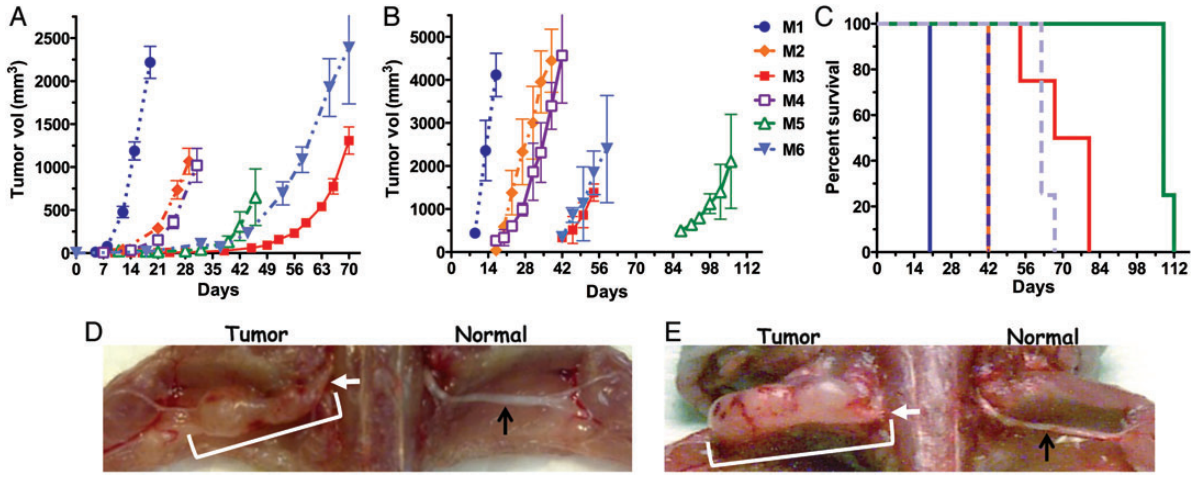

Fig. 1. Kinetics of MPNST growth. (A) Subcutaneous implantation of mouse MPNST cells (1×10^6, except for M1 [3×10^5] and M5 [3×10^6]; in Matrigel) in C57BL6/129SVSVImJ hybrid mice. Mice were sacrificed due to tumor size or ulceration. (B) Mouse MPNST cells (5×10^4) were implanted into the left sciatic nerve. (C) Survival of mice bearing sciatic nerve implants, from (B). (D) Mouse M2 cells (2.5×10^4) were implanted into the left sciatic nerve and mice were sacrificed on day 23. (E) Human S462 MSLCs (5×10^5) were implanted into the left sciatic nerve and athymic mice were sacrificed on day 127. White arrows indicate implantation site, white bracket the tumor, and black arrows are normal sciatic nerve on nonimplanted side.

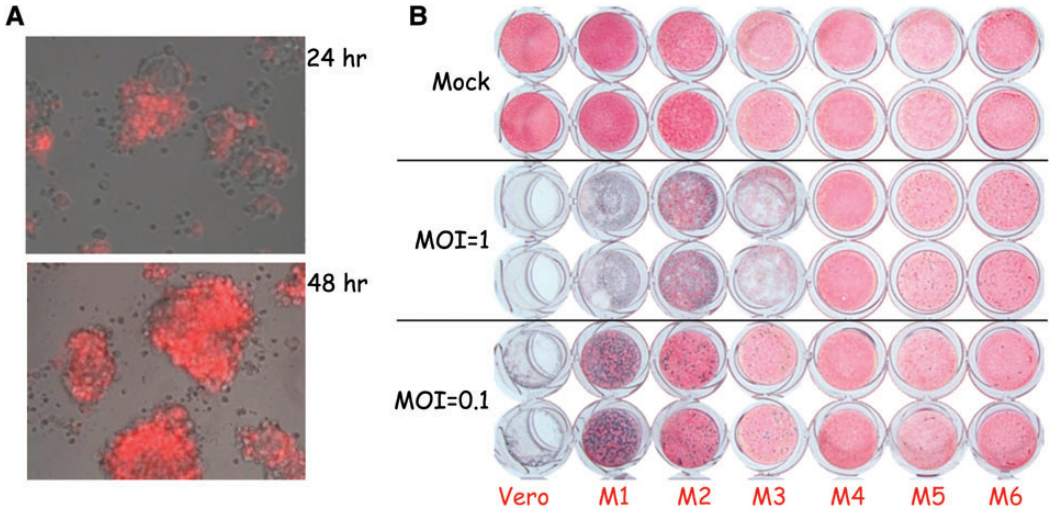

Fig. 2. Replication of G47Δ in MPNST cells. (A) Human S462 MSLCs infected with G47Δ-mCherry (multiplicity of infection [MOI] = 1) were imaged 24 and 48 h postinfection. Merged phase contrast–fluorescent images (infected cells are red). (B) Mouse MPNST cells (M1–M6) and Vero were infected with G47Δ at the indicated MOI or mock (PBS) (duplicate wells), fixed 3 days later, stained with X-Gal, and counterstained with Neutral Red. Vero cells are a highly susceptible cell line for comparison.

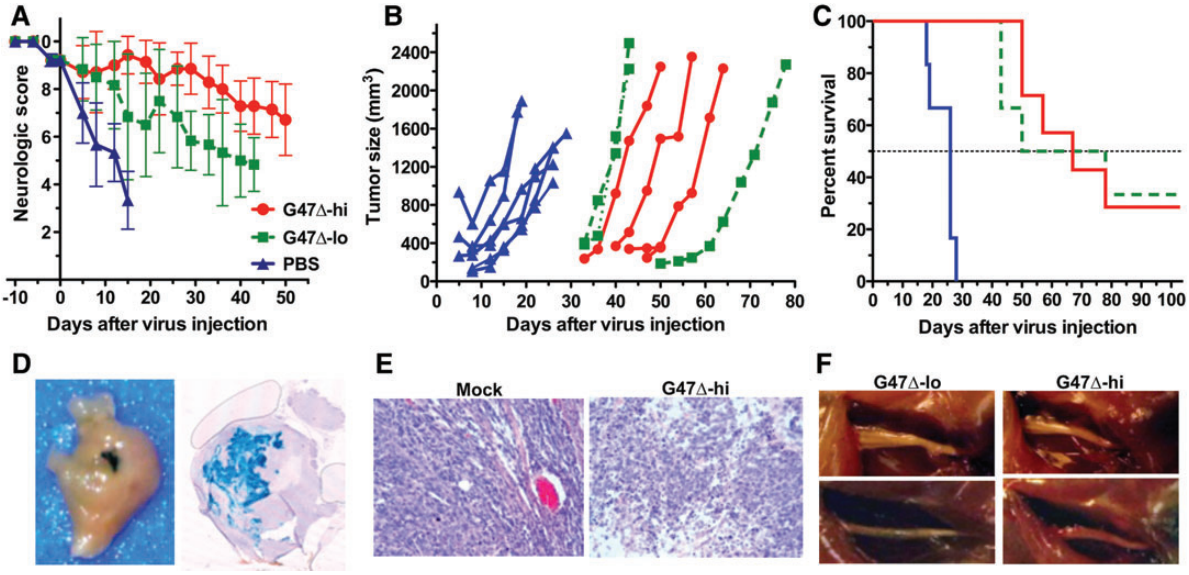

Fig. 3. Treatment of sciatic nerve human MSLC tumors. S462 MSLCs (1×10^5) were implanted into the sciatic nerve of athymic (nu/nu) mice. G47Δ-lo (2×10^5 pfu; $n = 6$), G47Δ-hi (2×10^6 pfu; $n = 7$), or PBS ($n = 6$) in 2 μL was injected on day 56. The mean internal diameters ± SD of the tumors at injection were: mock, 39 ± 5.0; G47Δ-lo, 35 ± 5.9; G47Δ-hi, 32 ± 8.3. (A) Mean neurologic score ± SD; $P < .05$ mock vs G47Δ-lo or -hi on days 5–15; G47Δ-hi vs G47Δ-lo on days 15, 19, 26–43. (B) Tumor growth for individual mice. Three mice in G47Δ-hi and -lo groups had undetectable tumors (<30 mm^3) and are not included. (C) Survival; $P < .002$ (log-rank test) G47Δ vs mock. Median survival was 23 days for mock and 64 days for G47Δ. One mouse in the G47Δ-lo group was found dead on day 30 and in the G47Δ-hi group due to obstruction on day 78 (no apparent tumors). Experiment was terminated on day 103 after virus injection. (D) Established tumors were intratumorally injected with G47Δ (3×10^6 in 2 μL), mice were sacrificed, and tumor was isolated 5 days later. Fixed tumor was stained by X-Gal histochemistry (infected cells stain blue). Left, whole tumor. Right, coronal section. (E) Histology (hematoxylin-eosin stain) of tumors treated on day 61 (PBS and G47Δ-hi) and harvested on day 68. (F) Tumor-bearing sciatic nerves after treatment (sacrifice on day 103). G47Δ-lo on left and G47Δ-hi on right.

S462 MSLCs were implanted into the sciatic nerve of athymic mice. When neurologic score decreased from 10 to 8 or 9 points, the tumor-bearing sciatic nerve was surgically exposed and a single injection of PBS or G47Δ was administered. Two G47Δ doses were compared, G47Δ-hi (2×10^6 plaque-forming units [pfu]) and 10-fold lower G47Δ-lo (2×10^5 pfu). In the PBS control group, all tumors exhibited rapid growth such that the mice had to be sacrificed before tumors were externally palpable in the G47Δ-treated groups (Fig. 3B). Virus spread within tumors was detected by X-Gal staining of G47Δ-infected cells. The

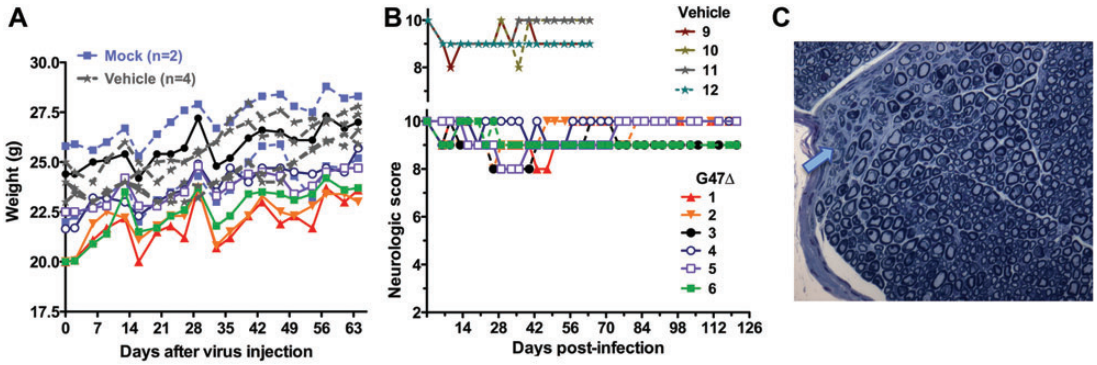

Fig. 4. Safety of G47Δ injection into sciatic nerve. G47Δ (2.5×10^6 pfu; $n = 6$) or PBS (vehicle; $n = 4$) in 2 μL was injected into the sciatic nerve of athymic mice (nu/nu). (A) Mice were weighed. Mock mice were not injected. (B) Neurologic score. Upper panel, vehicle injected. Lower panel, G47Δ injected. All G47Δ-treated mice, except 3 and 6, returned to scores of 10. The 2 mock mice had scores of 10 throughout. (C) Toluidine blue staining of 1-μm-thick sections of sciatic nerve from G47Δ-injected nerve, with arrow indicating the needle track.

G47Δ injection site is easily visible (Fig. 3D, left, blue), and sectioning through the tumor demonstrates efficient spread (Fig. 3D, right, blue) at 5 days postinjection. Histology of tumors harvested 7 days after G47Δ-hi injection showed large areas of necrosis compared with controls (Fig. 3E). While the decrease in neurologic score was significantly less in G47Δ-hi compared with G47Δ-lo (Fig. 3A), there was no difference in median survival between the treatment groups (Fig. 3C). However, both doses resulted in about 30% long-term survivors, compared with 0% in the PBS group, with the sciatic nerves from the surviving G47Δ-treated mice showing no tumor (Fig. 3F).

Safety of G47Δ After Sciatic Nerve Injection

In light of the significant efficacy exhibited in sciatic nerve tumors, we examined the safety of direct sciatic nerve injection of G47Δ. G47Δ (2.5×10^6 pfu) or PBS (vehicle) was injected into the normal left sciatic nerve of athymic mice without tumors. All G47Δ-injected mice gained weight over the observation period, which did not differ from that of the control vehicle-injected mice (Fig. 4A). Four G47Δ-injected mice experienced a transient small decrease in neurologic score that returned to normal (score = 10), while 2 mice exhibited a small deficit long term, similar to what was seen with the vehicle-injected mice (Fig. 4B). When the experiment was terminated (after 121 days for G47Δ and 70 days for vehicle), the injected left sciatic nerves and the noninjected right sciatic nerves were removed for histological evaluation using plastic embedded sections and electron microscopy examination. The G47Δ-injected sciatic nerves did not exhibit any ultrastructural abnormalities; there was no evidence of axonal loss, demyelination, axonal degeneration, or regenerating clusters compared with the noninjected sciatic nerves, with the exception of focal needle track damage that was also seen in the PBS-injected nerves (Fig. 4C, Supplementary Fig. S5).

Treatment of Immunocompetent MPNST Model

The sensitivity of the mouse MPNST cell lines to G47Δ varied over a large range. M1 was the most permissive, followed by M2 and M3, while M4 to M6 were relatively resistant (Fig. 2B). All cell lines were similarly sensitive to wild-type HSV-1[36] and expressed the herpesvirus entry mediator C (HveC; data not shown). We therefore decided to use M2 (G47Δ permissive but not too rapid tumor growth) to test treatment. M2 sciatic nerve tumors were apparent prior to treatment (Fig. 5A) in proximity to the axon bundles (Fig. 5B, white arrow). G47Δ was able to replicate and spread in the tumors, but not in the nerves, as illustrated by X-Gal staining of tumor sections 2 days postinjection (Fig. 5B, blue stain). Because of the rapid growth of the M2 tumors, we treated tumors with a single injection of G47Δ (3×10^6 pfu) or PBS on day 10. Compared with control, G47Δ treatment significantly delayed tumor growth (Fig. 5C), improved neurologic scores (Fig. 5D), and extended survival (Fig. 5E). While median survival increased only from 40 days for PBS to 51 days for G47Δ, importantly 30% of G47Δ-treated mice survived long term. The 5 surviving mice did not have macroscopically detectable tumor and exhibited good neurologic scores of 8–10. Histological examination of toluidine blue stained sections from treated sciatic nerves from 4 of these mice also revealed no evidence of tumor. In addition, the only ultrastructural abnormalities were areas of edema and some infiltration of lymphocytes and mast cells, which were also present in a mouse with a normal neurologic score of 10 (Supplementary Fig. S6).

Improved Antitumor Efficacy in Immunocompetent Models With "Armed" G47Δ

Expression of PF4 or IL-12 was previously shown not to alter the replication of G47Δ.[13,31] G47Δ-PF4 was previously tested in M2 subcutaneous tumors in immunodeficient mice and demonstrated significant but limited inhibition of tumor growth over G47Δ-empty.[13] Thus, we examined the in vivo efficacy of G47Δ-PF4 in M2 sciatic nerve tumors in immunocompetent mice. When the median neurologic score decreased to about 8 (day 11), the sciatic nerve was surgically exposed and G47Δ-PF4 or G47Δ-empty (no transgene) or mock was injected into the tumor, followed by a second injection on day 17. At the second injection, there was a significant increase in the internal tumor volume of PBS- versus virus-injected tumors (Fig. 6A). While both G47Δ-empty and G47Δ-PF4 significantly reduced tumor growth (data not shown) and neurologic deficit (Fig. 6B) compared with PBS, PF4 expression did not significantly

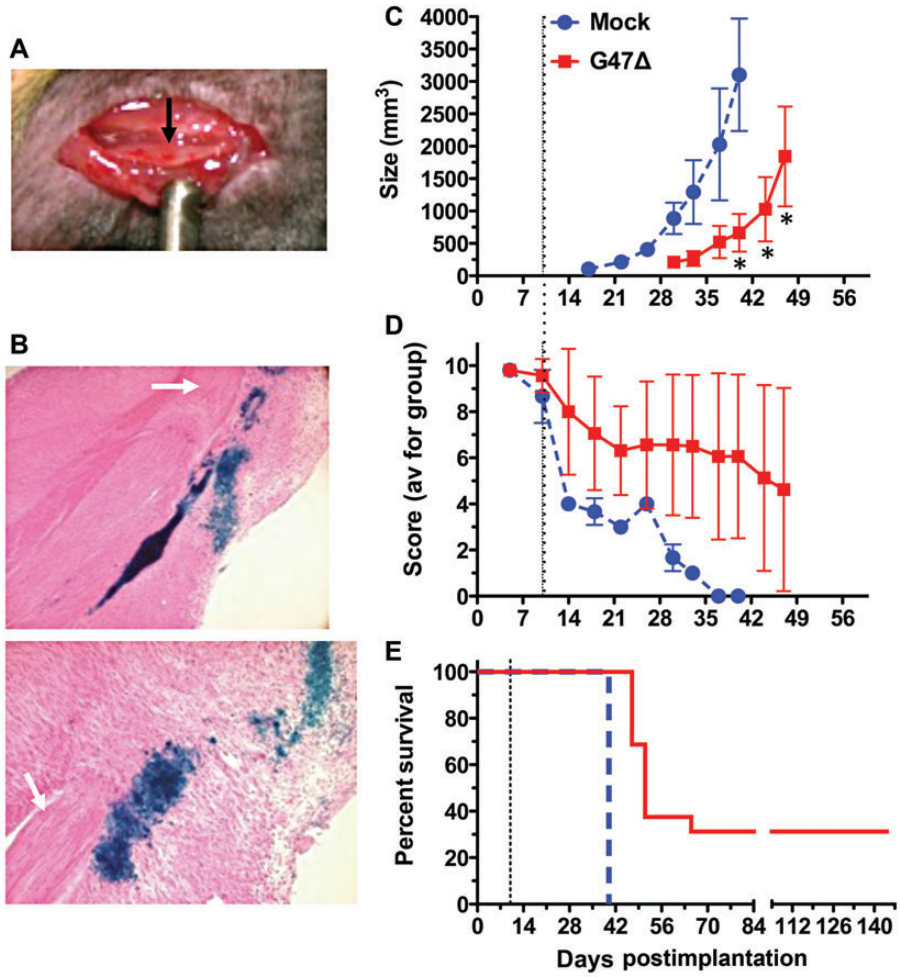

Fig. 5. Treatment of mouse sciatic nerve MPNST in immunocompetent mice. Mouse M2 cells (5×10^4) were implanted into the sciatic nerve of C57BL6/129SVSVImJ hybrid mice. (A) View of tumor in sciatic nerve 7 days postimplant (black arrow). (B) Tumors were injected with G47Δ (3×10^6 pfu) on day 10, and mice were sacrificed 48 h later. X-Gal staining of G47Δ-infected cells (blue) in sagittal sections from same tumor. Upper, 4× obj; lower 10× obj. Nerve bundle (white arrow). (C) G47Δ (3×10^6 pfu; $n = 16$) or PBS ($n = 4$) in 2 μL was injected on day 10 (dashed line). External tumor size was measured by caliper. *$P < .05$, unpaired t-test. (D) Neurologic score; $P < .01$, days 30–40; 2-way ANOVA (Bonferroni posttests). (E) Kaplan–Meier survival curve. $P < .0001$, log-rank test.

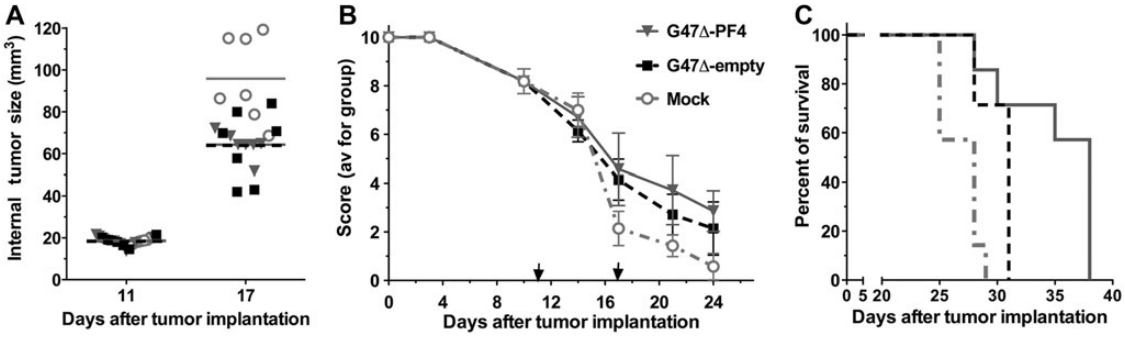

Fig. 6. G47Δ-PF4 treatment of sciatic nerve M2 tumors. Mouse M2 cells (5×10^4) were implanted into the sciatic nerve of C57BL6/129SVSVImJ hybrid mice. G47Δ-empty ($n = 7$), G47Δ-PF4 (2×10^7 pfu; $n = 7$), or PBS ($n = 7$) in 2 μL was injected on days 11 and 17 (arrows). (A) Tumor size was measured internally. On day 17, $P < .0001$ PBS vs treated. (B) Neurologic score; $P < .01$ PBS vs G47Δ-empty or G47Δ-PF4 on days 17, 21, and 24; $P > .1$ G47Δ-empty vs G47Δ-PF4. (C) Survival; $P < .01$ mock vs G47Δ-empty, $P < .005$ PBS vs G47Δ-PF4, $P < .05$ G47Δ-empty vs G47Δ-PF4.

alter these parameters. However, G47Δ-PF4 did significantly extend survival compared with G47Δ-empty (Fig. 6C), with median survival of 28, 31, and 38 days for PBS, G47Δ-empty, and G47Δ-PF4, respectively. In this experiment the M2 tumors grew very rapidly compared with those in Fig. 5, and treatment was initiated at a lower median neurologic score (8 vs 9), which may explain the difference in efficacy.

To examine the impact of IL-12 expression, we used M3 tumors, which grow more slowly than M2 (Fig. 1B). Treatment was initiated when the median neurologic score decreased to 8.4 (day 31 after implantation), with a second injection on day 6. Both G47Δ-empty and G47Δ–IL12 significantly inhibited tumor growth and decreased neurologic deficits compared with PBS (Fig. 7A and B). There were no externally measurable tumors in the G47Δ–IL12 treated group until day 17, compared with day 10 for the PBS and G47Δ-empty groups (Fig. 7B). G47Δ–IL12 was significantly better than G47Δ-empty in all outcome measures. The median survival was 21, 28, and 33 days after treatment for PBS, G47Δ-empty, and G47Δ–IL12, respectively, with 2 mice in the G47Δ–IL12 group surviving at least 9 weeks after treatment (Fig. 7C).

Discussion

The poor prognosis for patients with MPNST and the low efficacy of tested pharmacological agents makes it important to identify and evaluate new treatments for these tumors. Here we describe 2 new orthotopic MPNST models that we used to evaluate oHSV efficacy: (i) mouse MPNST cells, isolated from spontaneously arising tumors in NF-cis ($Nf1^{+/-}$/$Trp53^{+/-}$) transgenic mice,[10] implanted into the sciatic nerve of syngeneic immunocompetent mice; and (ii) human S462 MSLCs[20] implanted into the sciatic nerve of immunodeficient mice. In MPNST patients, the most common nerve of origin is the sciatic nerve.[39] The sciatic nerve in mice is surgically accessible and of sufficient size to accommodate tumor cell injection, and tumor growth/nerve damage can be evaluated clinically by hind-limb and paw deficits. The mouse MPNST cells varied significantly in their growth kinetics, after both subcutaneous or sciatic nerve implantation. Subcutaneous implantation in nude mice revealed similar growth kinetics to implantation in immunocompetent mice, with M1 being the fastest and M3 the slowest (data not shown). The only major difference after sciatic nerve implantation was the extremely slow growth of M5. The human MSLCs formed sciatic nerve tumors more slowly than the mouse cells. This is the first description of a cancer stem cell–like peripheral nerve tumor xenograft model. Recently, a sciatic nerve human MPNST model was used to demonstrate the effectiveness of tamoxifen.[40] Tumor-initiating cells have been isolated from MPNST arising in transgenic $Nf1^{+/-}$/$Ink4a/Arf^{-/-}$ mice with very high frequency.[41] Whether these cells have stemlike properties or how similar they are to our human MSLCs is unknown. Human MSLCs are extremely difficult to isolate (M. Spyra and V. F. Mautner, unpublished data), and there are only a few human MPNST cell lines that are tumorigenic.[42,43]

HSV is a neurotrophic virus, which after footpad inoculation of wild-type virus invades the CNS via the sciatic nerve, causing paralysis and death.[44] Direct injection of wild-type HSV into the sciatic nerve causes demyelination and inflammation at early time points, followed by lethal encephalitis.[45–47] Oncolytic HSVs, such as G207 and G47Δ, are engineered to minimize neurotoxicity[27,48] and thus should be appropriate for treating peripheral nerve tumors or tumors invading peripheral nerves. There are several ongoing clinical trials using oHSV as a single therapeutic agent against a variety of tumors, with no evidence of adverse events and indications of efficacy.[24] We found that injection of G47Δ into the sciatic nerves of HSV-sensitive immunodeficient athymic mice was nonpathogenic, with mice exhibiting similar minor, transient neurologic deficits and needle track damage as the PBS-injected mice. Sciatic nerves from G47Δ-treated tumors in "cured" immunocompetent mice did not exhibit virus pathology. A different oHSV expressing IL-12 (MOO2) was recently found to be safe after intracerebral injection in susceptible nonhuman primates.[49] Many solid tumors, such as prostate and pancreatic cancers, have a propensity for neural invasion that is often associated with poor outcomes.[50] In a previous model of peripheral nerve sheath tumors, human neuroblastoma cells were implanted into the sciatic nerve. A single intratumoral injection of G207, when mice exhibited hind-limb dysfunction, delayed functional decline and prolonged survival.[46] Oncolytic HSV NV1023 was shown to effectively treat mice implanted with human pancreatic and prostate cancer cells in the sciatic nerve while preserving nerve function.[47,51] Here we describe the first successful

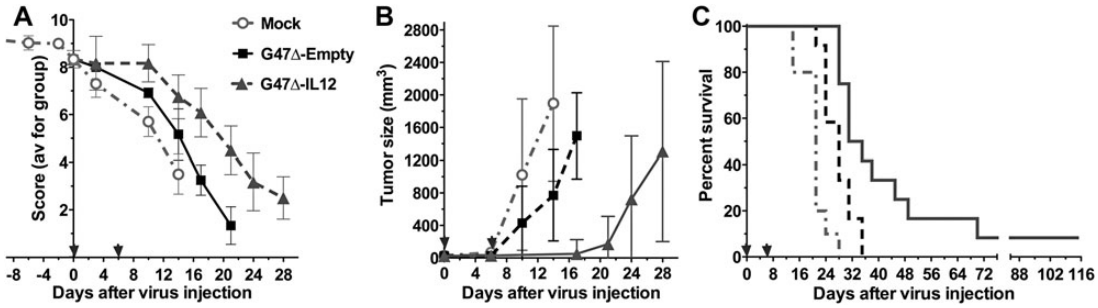

Fig. 7. G47Δ–IL12 treatment of sciatic nerve M3 tumors. Mouse M3 cells (5×10^4) were implanted into the sciatic nerve of C57BL6/129SVSVImJ hybrid mice. G47Δ-empty ($n = 12$), G47Δ–IL12 ($n = 12$) (9×10^5 pfu), or PBS ($n = 10$) in 2 μL was injected on days 0 (31 days after implantation) and 6 (arrows). Data are combined from 2 experiments. (A) Neurologic score; $P < .01$ mock vs G47Δ-empty or G47Δ–IL12 on days 10 and 14, $P < .001$ G47Δ-empty vs G47Δ–IL12 on days 14–21 (unpaired *t*-test). (B) Tumor size. In the G47Δ–IL12 group, there were no tumors measurable externally on days 10 and 14. $P < .003$, PBS vs G47Δ-empty on day 14, $P < .0001$ G47Δ–IL12 vs G47Δ-empty on day 17 (unpaired *t*-test). (C) Survival; $P < .005$ mock vs G47Δ-empty and G47Δ–IL12, and G47Δ–IL12 vs G47Δ-empty.

treatment of orthotopic MPNST implant models with oHSV. Novel features of our 2 sciatic nerve models are the use of mouse MPNST in immunocompetent mice and human MSLCs in nude mice. We developed a neurologic scoring scheme for hind-limb deficit, which allowed us to monitor tumor growth prior to externally discernible tumors.

A number of oHSV vectors have been evaluated by us and others in various MPNST models. The Cripe laboratory has tested the anti-MPNST activity of different oHSVs in immunodeficient mice bearing subcutaneous or intraperitoneal human MPNST xenografts.[42,52,53] For example, in a subcutaneous model with S462.TY cells, similar to the MSLC parental cells, treatment with a G207-equivalent oHSV increased survival by about 25%.[52] In this model, an armed oHSV-expressing tissue inhibitor of matrix metalloproteinase 3 (rQT3) further extended survival more than 2-fold.[52] We previously described the treatment of subcutaneously implanted mouse M2 tumors in immunodeficient mice with "armed" G47Δ expressing dominant-negative FGF receptor (dnFGFR) or PF4.[12,13] G47Δ alone inhibited tumor growth to a small but significant extent, whereas transgene expression (dnFGFR or PF4) further inhibited tumor growth, which was associated with a >4-fold decrease in microvascular density.[12,13] Here, we found that G47Δ was more efficacious in the M2 immunocompetent sciatic nerve model, with about a third of the treated mice surviving long term. This suggests possible immune-mediated effects, as have been reported for oHSV in other mouse syngeneic models.[54–57] PF4 expression prolonged survival in the M2 model compared with G47Δ-empty. In the mouse M3 model, immunomodulatory IL-12 expression increased oHSV efficacy; reducing the rate of neurologic decline, delaying tumor growth, and extending survival. G47Δ–IL12 was also shown to prolong survival in a syngeneic glioblastoma stem cell tumor model, with IL-12 expression in the tumor inducing IFN-γ synthesis.[31] Thus arming G47Δ with PF4 or IL12 transgenes improved antitumor efficacy in immunocompetent MPNST models, with IL-12 producing a small number of long-term survivors.

In conclusion, we demonstrate the efficacy of oHSV G47Δ in the treatment of both human and mouse syngeneic orthotopic MPNST models and its lack of pathogenicity after sciatic nerve injection. G47Δ has previously been shown to effectively treat breast, prostate, and rectal carcinomas[30,58,59] and thus should be considered for the treatment of patients with neural invasion of these cancers. Human MSLC implantation into the sciatic nerve provides a new representative MPNST model that should be very useful in testing novel therapeutics for MPNST. The orthotopic immunocompetent MPNST model will be of great value in testing immunotherapeutic strategies for this debilitating tumor, which is often metastatic, and complement the use of genetically engineered mouse models.[9] The enhanced efficacy of G47Δ–IL12 in this model indicates that other immunotherapies for MPNST, as well as combinations with immunogenic chemotherapy, should be evaluated, and provides compelling support for clinical translation.

Supplementary Material

Supplementary material is available online at *Neuro-Oncology* (http://neuro-oncology.oxfordjournals.org/).

Funding

This research was supported in part by grants from the Department of Defense Neurofibromatosis Program (W81XWH-07-0359 to S.D.R. and W81XWH-10-1-0091 to S.A.) and from the Bundesministerium für Bildung und Forschung (BMBF 01GM0804 to A.K. and V.F.M.).

Acknowledgments

We thank Melissa Humphreys for technical assistance and Martin Selig (Diagnostic EM Unit, MGH Pathology) for assistance with the electron microscopy.

Conflict of interest statement. S.R.D. and R.L.M. are named inventors on patents relating to oncolytic herpes simplex viruses, which were filed by Georgetown University and Massachusetts General Hospital.

References

1. Grobmyer SR, Reith JD, Shahlaee A, et al. Malignant peripheral nerve sheath tumor: molecular pathogenesis and current management considerations. *J Surg Oncol*. 2008;97:340–349.
2. Zou C, Smith KD, Liu J, et al. Clinical, pathological, and molecular variables predictive of malignant peripheral nerve sheath tumor outcome. *Ann Surg*. 2009;249:1014–1022.
3. Kroep JR, Ouali M, Gelderblom H, et al. First-line chemotherapy for malignant peripheral nerve sheath tumor (MPNST) versus other histological soft tissue sarcoma subtypes and as a prognostic factor for MPNST: an EORTC soft tissue and bone sarcoma group study. *Ann Oncol*. 2011;22:207–214.
4. Widemann BC. Current status of sporadic and neurofibromatosis type 1–associated malignant peripheral nerve sheath tumors. *Curr Oncol Rep*. 2009;11:322–328.
5. Kolberg M, Holand M, Agesen TH, et al. Survival meta-analyses for >1800 malignant peripheral nerve sheath tumor patients with and without neurofibromatosis type 1. *Neuro Oncol*. 2013;15:135–147.
6. Porter DE, Prasad V, Foster L, et al. Survival in malignant peripheral nerve sheath tumours: a comparison between sporadic and neurofibromatosis type 1–associated tumours. *Sarcoma*. 2009;2009:Article ID 756395.
7. Gottfried ON, Viskochil DH, Couldwell WT. Neurofibromatosis type 1 and tumorigenesis: molecular mechanisms and therapeutic implications. *Neurosurg Focus*. 2010;28:E8.
8. Upadhyaya M, Kluwe L, Spurlock G, et al. Germline and somatic NF1 gene mutation spectrum in NF1-associated malignant peripheral nerve sheath tumors (MPNSTs). *Hum Mutat*. 2008;29:74–82.
9. Brossier NM, Carroll SL. Genetically engineered mouse models shed new light on the pathogenesis of neurofibromatosis type I–related neoplasms of the peripheral nervous system. *Brain Res Bull*. 2012;88:58–71.
10. Vogel KS, Klesse LJ, Velasco-Miguel S, et al. Mouse tumor model for neurofibromatosis type 1. *Science*. 1999;286:2176–2179.
11. Cichowski K, Shih TS, Schmitt E, et al. Mouse models of tumor development in neurofibromatosis type 1. *Science*. 1999;286:2172–2176.
12. Liu TC, Zhang T, Fukuhara H, et al. Dominant-negative fibroblast growth factor receptor expression enhances antitumoral potency

of oncolytic herpes simplex virus in neural tumors. *Clin Cancer Res*. 2006;12:6791–6799.

13. Liu TC, Zhang T, Fukuhara H, et al. Oncolytic HSV armed with platelet factor 4, an antiangiogenic agent, shows enhanced efficacy. *Mol Ther*. 2006;14:789–797.
14. Clevers H. The cancer stem cell: premises, promises and challenges. *Nat Med*. 2011;17:313–319.
15. Suva ML, Riggi N, Stehle JC, et al. Identification of cancer stem cells in Ewing's sarcoma. *Cancer Res*. 2009;69:1776–1781.
16. Walter D, Satheesha S, Albrecht P, et al. CD133 positive embryonal rhabdomyosarcoma stem-like cell population is enriched in rhabdospheres. *PLoS One*. 2011;6:e19506.
17. Stratford EW, Castro R, Wennerstrom A, et al. Liposarcoma cells with Aldefluor and CD133 activity have a cancer stem cell potential. *Clin Sarcoma Res*. 2011;1:8.
18. Martins-Neves SR, Lopes AO, do Carmo A, et al. Therapeutic implications of an enriched cancer stem-like cell population in a human osteosarcoma cell line. *BMC Cancer*. 2012;12:139.
19. Salerno M, Avnet S, Bonuccelli G, et al. Sphere-forming cell subsets with cancer stem cell properties in human musculoskeletal sarcomas. *Int J Oncol*. 2013;43:95–102.
20. Spyra M, Kluwe L, Hagel C, et al. Cancer stem cell-like cells derived from malignant peripheral nerve sheath tumors. *PLoS One*. 2011;6:e21099.
21. Varghese S, Rabkin SD. Oncolytic herpes simplex virus vectors for cancer virotherapy. *Cancer Gene Ther*. 2002;9:967–978.
22. Todo T. Active immunotherapy: oncolytic virus therapy using HSV-1. *Adv Exp Med Biol*. 2012;746:178–186.
23. Friedman GK, Pressey JG, Reddy AT, et al. Herpes simplex virus oncolytic therapy for pediatric malignancies. *Mol Ther*. 2009;17:1125–1135.
24. Kaur B, Chiocca EA, Cripe TP. Oncolytic HSV-1 virotherapy: Clinical experience and opportunities for progress. *Curr Pharm Biotechnol*. 2012;13:1842–1851.
25. Jeyaretna DS, Kuroda T. Recent advances in the development of oncolytic HSV-1 vectors: "arming" of HSV-1 vectors and application of bacterial artificial chromosome technology for their construction. *Curr Opin Mol Ther*. 2007;9:447–466.
26. Kaur B, Cripe TP, Chiocca EA. "Buy one get one free": armed viruses for the treatment of cancer cells and their microenvironment. *Curr Gene Ther*. 2009;9:341–355.
27. Todo T, Martuza RL, Rabkin SD, et al. Oncolytic herpes simplex virus vector with enhanced MHC class I presentation and tumor cell killing. *Proc Natl Acad Sci U S A*. 2001;98:6396–6401.
28. Prabhakar S, Messerli SM, Stemmer-Rachamimov AO, et al. Treatment of implantable NF2 schwannoma tumor models with oncolytic herpes simplex virus G47Delta. *Cancer Gene Ther*. 2007;14:460–467.
29. Wakimoto H, Kesari S, Farrell CJ, et al. Human glioblastoma-derived cancer stem cells: establishment of invasive glioma models and treatment with oncolytic herpes simplex virus vectors. *Cancer Res*. 2009;69:3472–3481.
30. Li J, Zeng W, Huang Y, et al. Treatment of breast cancer stem cells with oncolytic herpes simplex virus. *Cancer Gene Ther*. 2012;19:707–714.
31. Cheema TA, Wakimoto H, Fecci PE, et al. Multifaceted oncolytic virus therapy for glioblastoma in an immunocompetent cancer stem cell model. *Proc Natl Acad Sci U S A*. 2013;110:12006–12011.
32. Del Vecchio M, Bajetta E, Canova S, et al. Interleukin-12: biological properties and clinical application. *Clin Cancer Res*. 2007;13:4677–4685.
33. Lippi G, Favaloro EJ. Recombinant platelet factor 4: a therapeutic, anti-neoplastic chimera? *Semin Thromb Hemost*. 2010;36:558–569.
34. Aidoudi S, Bikfalvi A. Interaction of PF4 (CXCL4) with the vasculature: a role in atherosclerosis and angiogenesis. *Thromb Haemost*. 2010;104:941–948.
35. Li H, Velasco-Miguel S, Vass WC, et al. Epidermal growth factor receptor signaling pathways are associated with tumorigenesis in the Nf1:p53 mouse tumor model. *Cancer Res*. 2002;62:4507–4513.
36. Farassati F, Pan W, Yamoutpour F, et al. Ras signaling influences permissiveness of malignant peripheral nerve sheath tumor cells to oncolytic herpes. *Am J Pathol*. 2008;173:1861–1872.
37. Kanai R, Rabkin SD, Yip S, et al. Oncolytic virus-mediated manipulation of DNA damage responses: synergy with chemotherapy in killing glioblastoma stem cells. *J Natl Cancer Inst*. 2012;104:42–55.
38. Kuroda T, Martuza RL, Todo T, et al. Flip-Flop HSV-BAC: bacterial artificial chromosome based system for rapid generation of recombinant herpes simplex virus vectors using two independent site-specific recombinases. *BMC Biotechnol*. 2006;6:40.
39. Ducatman BS, Scheithauer BW, Piepgras DG, et al. Malignant peripheral nerve sheath tumors. A clinicopathologic study of 120 cases. *Cancer*. 1986;57:2006–2021.
40. Byer SJ, Eckert JM, Brossier NM, et al. Tamoxifen inhibits malignant peripheral nerve sheath tumor growth in an estrogen receptor-independent manner. *Neuro Oncol*. 2011;13:28–41.
41. Buchstaller J, McKeever PE, Morrison SJ. Tumorigenic cells are common in mouse MPNSTs but their frequency depends upon tumor genotype and assay conditions. *Cancer Cell*. 2012;21:240–252.
42. Mahller YY, Vaikunth SS, Currier MA, et al. Oncolytic HSV and erlotinib inhibit tumor growth and angiogenesis in a novel malignant peripheral nerve sheath tumor xenograft model. *Mol Ther*. 2007;15:279–286.
43. Miller SJ, Rangwala F, Williams J, et al. Large-scale molecular comparison of human schwann cells to malignant peripheral nerve sheath tumor cell lines and tissues. *Cancer Res*. 2006;66:2584–2591.
44. Wildy P. The progression of herpes simplex virus to the central nervous system of the mouse. *J Hyg (Lond)*. 1967;65:173–192.
45. Townsend JJ, Collins PK. Peripheral nervous system demyelination with herpes simplex virus. *J Neuropathol Exp Neurol*. 1986;45:419–425.
46. Mashour GA, Moulding HD, Chahlavi A, et al. Therapeutic efficacy of G207 in a novel peripheral nerve sheath tumor model. *Exp Neurol*. 2001;169:64–71.
47. Gil Z, Rein A, Brader P, et al. Nerve-sparing therapy with oncolytic herpes virus for cancers with neural invasion. *Clin Cancer Res*. 2007;13:6479–6485.
48. Sundaresan P, Hunter WD, Martuza RL, et al. Attenuated, replication-competent herpes simplex virus type 1 mutant G207: safety evaluation in mice. *J Virol*. 2000;74:3832–3841.
49. Markert JM, Cody JJ, Parker JN, et al. Preclinical evaluation of a genetically engineered herpes simplex virus expressing interleukin-12. *J Virol*. 2012;86:5304–5313.
50. Chatterjee D, Katz MH, Rashid A, et al. Perineural and intraneural invasion in posttherapy pancreaticoduodenectomy specimens

predicts poor prognosis in patients with pancreatic ductal adenocarcinoma. *Am J Surg Pathol*. 2012;36:409–417.

51. Kelly K, Brader P, Rein A, et al. Attenuated multimutated herpes simplex virus-1 effectively treats prostate carcinomas with neural invasion while preserving nerve function. *FASEB J*. 2008;22:1839–1848.
52. Mahller YY, Vaikunth SS, Ripberger MC, et al. Tissue inhibitor of metalloproteinase-3 via oncolytic herpesvirus inhibits tumor growth and vascular progenitors. *Cancer Res*. 2008;68:1170–1179.
53. Maldonado AR, Klanke C, Jegga AG, et al. Molecular engineering and validation of an oncolytic herpes simplex virus type 1 transcriptionally targeted to midkine-positive tumors. *J Gene Med*. 2010;12:613–623.
54. Toda M, Rabkin SD, Kojima H, et al. Herpes simplex virus as an in situ cancer vaccine for the induction of specific anti-tumor immunity. *Hum Gene Ther*. 1999;10:385–393.
55. Miller CG, Fraser NW. Role of the immune response during neuro-attenuated herpes simplex virus-mediated tumor destruction in a murine intracranial melanoma model. *Cancer Res*. 2000;60:5714–5722.
56. Li H, Dutuor A, Tao L, et al. Virotherapy with a type 2 herpes simplex virus-derived oncolytic virus induces potent antitumor immunity against neuroblastoma. *Clin Cancer Res*. 2007;13:316–322.
57. Farrell CJ, Zaupa C, Barnard Z, et al. Combination immunotherapy for tumors via sequential intratumoral injections of oncolytic herpes simplex virus 1 and immature dendritic cells. *Clin Cancer Res*. 2008;14:7711–7716.
58. Fukuhara H, Martuza RL, Rabkin SD, et al. Oncolytic herpes simplex virus vector g47delta in combination with androgen ablation for the treatment of human prostate adenocarcinoma. *Clin Cancer Res*. 2005;11:7886–7890.
59. Kolodkin-Gal D, Edden Y, Hartshtark Z, et al. Herpes simplex virus delivery to orthotopic rectal carcinoma results in an efficient and selective antitumor effect. *Gene Ther*. 2009;16:905–915.